Published in final edited form as:
J Neurochem. 2010 October ; 115(1): 220–233. doi:10.1111/j.1471-4159.2010.06920.x.

Neurosteroid transport by the organic solute transporter OSTα-OSTβ

Fang Fang[*], **Whitney V. Christian**[*], **Sadie G. Gorman**[*], **Mei Cui**[†], **Jiaoti Huang**[‡], **Kim Tieu**[†], and **Nazzareno Ballatori**[*]

[*]Department of Environmental Medicine, University of Rochester School of Medicine, Rochester, New York, USA

[†]Department of Neurology, University of Rochester School of Medicine, Rochester, New York, USA

[‡]Department of Pathology, University of Rochester School of Medicine, Rochester, New York, USA

Abstract

A variety of steroids, including pregnenolone sulfate (PREGS) and dehydroepiandrosterone sulfate (DHEAS) are synthesized by specific brain cells, and are then delivered to their target sites, where they exert potent effects on neuronal excitability. The present results demonstrate that [^{3}H]DHEAS and [^{3}H]PREGS are relatively high affinity substrates for the organic solute transporter, OSTα–OSTβ, and that the two proteins that constitute this transporter are selectively localized to steroidogenic cells in the cerebellum and hippocampus, namely the Purkinje cells and cells in the CA region in both mouse and human brain. Analysis of *Ost*α and *Ost*β mRNA levels in mouse Purkinje and hippocampal cells isolated via laser capture microdissection supported these findings. In addition, *Ost*α-deficient mice exhibited changes in serum dehydroepiandrosterone (DHEA) and DHEAS levels, and in tissue distribution of administered [^{3}H]DHEAS. OSTα and OSTβ proteins were also localized to the *zona reticularis* of human adrenal gland, the major region for DHEAS production in the periphery. These results demonstrate that OSTα-OSTβ is localized to steroidogenic cells of the brain and adrenal gland, and that it modulates DHEA/DHEAS homeostasis, suggesting that it may contribute to neurosteroid action.

Keywords

Organic solute transporter; neurosteroid transport; pregnenolone sulfate; dehydroepiandrosterone sulfate; Purkinje cells; CA region of the hippocampus

Introduction

Pregnenolone, progesterone, dehydroepiandrosterone (DHEA), and many other neuroactive steroids can be synthesized *de novo* in neuronal tissue, and thus are referred to as neurosteroids (Corpéchot et al. 1981, 1983; Do Rego et al. 2009; Mellon et al. 2001; Mellon 2007; Tsutsui 2008). Neurosteroids function not only as transcriptional activators for the

Address correspondence to Ned Ballatori, Ph.D., Department of Environmental Medicine, Box EHSC, University of Rochester School of Medicine, 601 Elmwood Ave., Rochester, NY 14642, Tel. 585-275-0262, Fax 585-256-2591, Ned_Ballatori@urmc.rochester.edu. Jiaoti Huang, M.D., Ph.D. is now Professor of Pathology and Director of Urologic Pathology in the Department of Pathology and Laboratory Medicine, David Geffen School of Medicine at UCLA. Tel. 310-267-2264, JiaotiHuang@mednet.ucla.edu

The authors affirm that there are no conflicts of interest.

regulation of gene expression, but they can also produce immediate and profound effects on neuronal excitability by interacting with specific cell surface neurotransmitter receptors, including both the major inhibitory neurotransmitter receptors, the γ-aminobutyric acid A ($GABA_A$) receptors, and the major excitatory neurotransmitter receptors, the N-methyl-d-aspartate (NMDA) receptors (Mellon et al. 2001). These interactions have been implicated in nerve cell proliferation, differentiation, activity, and survival, and in the control of a number of behavioral, neuroendocrine, and metabolic processes, including locomotor and sexual activity, aggressiveness, anxiety, and depression (Mellon et al. 2001; Mellon 2007; Flood and Roberts 1988). Treatment with physiological or pharmacologic concentrations of neurosteroids has been shown to promote nervous system development as well as improve learning and spatial memory, and there is growing evidence that imbalances in neurosteroid levels may contribute to the pathophysiology of affective disorders (Akwa et al. 2001; Eser et al. 2006; Flood and Roberts 1988; Flood et al. 1995; Isaacson et al. 1995; Maninger et al. 2009; Mellon 2007; Stoffel-Wagner 2003).

Two important excitatory neurosteroids are DHEA sulfate (DHEAS) and pregnenolone sulfate (PREGS) (Flood et al. 1995; Majewska et al. 1990; Mellon et al. 2001; Park-Chung et al. 1997; Schumacher et al. 2008). These sulfated neurosteroids, and in particular PREGS, have been shown to negatively modulate the $GABA_A$ receptors (Majewska et al. 1990) and positively modulate the NMDA subtype of glutamate receptors (Park-Chung et al. 1997). Thus, they may increase neuronal activity by inverse modulation of two different neurotransmitter receptors.

Neurosteroids are synthesized in neurons of the cerebellum, cortex, and hippocampus, as well as in astrocytes and oligodendrocytes (Do Rego et al. 2009; Kimoto et al. 2001; Mellon and Deschepper 1993; Tsutsui 2008; Ukena et al. 1998; Zwain and Yen 1999), and are then exported from these cells and delivered to their target sites. Bortfeld *et al*. (2006) suggested that MRP8/ABCC11 contributes to DHEAS efflux in axons; however, the contribution of this or other transporters to DHEAS export from brain cells has not yet been established.

In the human peripheral circulation, DHEAS is secreted solely by the adrenal gland, and its blood concentration is relatively high when compared to that of other steroids (i.e., 1–5 μM: Dharia and Parker 2004; Rainey and Nakamura 2008). The transporters responsible for moving DHEAS across adrenal gland cell membranes have also not been identified, although a potential role has been proposed for some members of the ATP-binding cassette (ABC) superfamily of proteins, including ABCC1, ABCC4, ABCC11 and ABCG2, as well as OAT3/SLC22A8, OAT4/SLC22A11, and OATP-B/SLC21A9 (Asif et al. 2005; Chen et al. 2005; Nozaki et al. 2007; Pizzagalli et al. 2003; Suzuki et al. 2003; Zelcer et al. 2003).

The present study examined the hypothesis that the recently identified heteromeric organic solute and steroid transporter, OSTα–OSTβ, is expressed in steroidogenic cells and that it contributes to the transport of conjugated neurosteroids. This hypothesis was suggested by several lines of evidence, including the observations that: (a) OSTα-OSTβ mediates the transport of conjugated steroids, including estrone-3 sulfate and DHEAS (Ballatori et al. 2005; Seward et al. 2003); (b) transport occurs by a facilitated diffusion mechanism, and thus OSTα-OSTβ can mediate either efflux or uptake depending on the electrochemical gradient of a given substrate (Ballatori et al. 2005); (c) *OST*α and *OST*β mRNAs are widely expressed in human tissues, including the brain and adrenal gland (Seward et al. 2003); and (d) both OSTα and OSTβ proteins are localized to the basolateral plasma membrane of cells that are known to export sterols, and in particular the liver, kidney and intestine (Seward et al. 2003; Dawson et al. 2005).

The present results demonstrate that PREGS and DHEAS are high-affinity substrates of OSTα–OSTβ; that these two proteins are expressed in the specific brain and adrenal gland cells that are thought to be involved in steroidogenesis; and that *Ostα*-deficient mice exhibit altered serum DHEA and DHEAS levels, as well as altered [^{3}H]DHEAS distribution. Taken together, the findings are consistent with the hypothesis that OSTα-OSTβ is involved in neurosteroid transport.

Experimental procedures

Materials and animals

[6,7-^{3}H(N)]Estrone 3-sulfate (57.3 Ci/mmol), [1,2,6,7-^{3}H(N)] DHEA(63 Ci/mmol), [1,2,6,7-^{3}H(N)] DHEAS (74 Ci/mmol) and [7-^{3}H(N)] PREG (12.6 Ci/mmol) were purchased from PerkinElmer Life and Analytical Sciences, Inc. (Boston, MA). [7-^{3}H(N)] PREGS (20 Ci/mmol) was purchased from American Radiolabeled Chemicals, Inc. (Saint Louis, MO). Antibodies to mouse Ostα (mA315) and Ostβ (mB91), and human OSTα (hA327) and OSTβ (hB1) have been described previously (Ballatori et al. 2005). Mouse monoclonal IP3R1 antibody was purchased from UC Davis/NeuroMab facility (Davis, CA). Mouse monoclonal NeuN antibody was obtained from Chemicon (Billerica, MA). All other chemicals and reagents were purchased from Ambion, Amersham Biosciences, Biorad, Fermentas, Integrated DNA Technologies, Invitrogen, Jackson Immunology Research Lab, J. T., Baker Inc., New England Biolab, Qiagen, Sigma-Aldrich, or Stratagene.

Ostα$^{-/-}$ mice were generated as previously described (Li et al. 2007; Ballatori et al. 2008). Animals were maintained on a standard laboratory diet (LabDiet 5010, PMI Nutrition International, Saint Louis, MO) at the University of Rochester School of Medicine and Dentistry Vivarium. Mouse genotyping was performed by PCR analysis of DNA isolated from tail biopsies, as previously described (Ballatori et al. 2008). Mature *Xenopus laevis* were purchased from Nasco (Fort Atkinson, WI) and were maintained under a 12 h light cycle at a room temperature of 18 °C in an animal facility located at the University of Rochester School of Medicine. All experimental protocols were approved by the local Animal Care and Use Committee, according to criteria outlined in the “Guide for the Care and Use of Laboratory Animals” prepared by the National Academy of Sciences, as published by the National Institutes of Health (NIH publication 86-23, revised 1985).

Xenopus laevis oocyte isolation and injection, and transport experiments

Isolation of *Xenopus laevis* oocytes was performed as described by Goldin (1992) and previously employed in our laboratory (Seward et al. 2003; Ballatori et al. 2005). Defolliculated stage V and VI oocytes were selected and injected with 50 nl of a solution containing *Ostα* and *Ostβ* cRNA (1 ng/gene per oocyte), or sterile water. Injected oocytes were cultured at 18°C with a daily change of modified Barth's media [88 mM NaCl, 1 mM KCl, 2.4 mM $NaHCO_3$, 0.82 mM $MgSO_4$, 0.33 mM $Ca(NO_3)_2$, 0.41 mM $CaCl_2$, and 20 mM HEPES-Tris, (pH 7.5)] supplemented with gentamycin (0.5 mg/ml). Oocytes with a homogeneous brown animal half and distinct equator line were selected for transport experiments 3 days post-injection.

To measure uptake of [^{3}H]DHEA, [^{3}H]DHEAS, [^{3}H]PREG, and [^{3}H]PREGS, control and cRNA-injected oocytes were incubated at 25°C for 5 min in 100 µl of modified Barth's solution in the presence of 1 µM of these compounds. In the kinetic studies, control or cRNA-injected oocytes were incubated with [^{3}H]PREGS or [^{3}H]DHEAS at concentrations of 0.1, 0.33, 1, 3.3, 10, 50, 100, 200, 400, and 800µM, and uptake was measured for 5 min at 25°C. In the *cis*-inhibition experiments, control or cRNA-injected oocytes were incubated at 25°C in 100 µl of modified Barth's solution in the presence of 50 nM [^{3}H]estrone 3-sulfate,

with or without other potential substrates/inhibitors. Uptake was stopped by rapid dilution with 2.5 ml of ice-cold modified Barth's solution, followed by three washes with this same solution. Two oocytes were placed in a polypropylene scintillation vial and dissolved in 200 µl of 10% SDS. Five ml of Opti-Fluor (Perkin-Elmer, Life and Analytical Sciences) scintillation cocktail was added, and samples were counted in a Beckman LS 6500 scintillation counter (Beckman Coulter, Fullerton, CA).

Quantitative reverse transcriptase (RT)-PCR analysis of mRNA levels in human and mouse tissues

Human adult normal tissue total RNAs were purchased from Biochain (Hayward, CA). Mouse tissue total RNAs were isolated as described previously (Ballatori et al. 2008) from adult mice of both genders. Synthetic oligonucleotide primers were designed (Table 1), and relative gene expression was determined on a Corbett Rotor-Gene 3000 real-time cycler (San Francisco, CA). All samples were analyzed in triplicate using BioRad's iScript™ One-step RT-PCR kit with SYBR Green (catalog no. 170–8893; Hercules, CA). Expression levels are reported as a ratio to *GAPDH/Gapdh*.

For the analysis of hepatic expression of some of the key genes involved in cholesterol and steroid homeostasis total RNA was isolated from adult wild type and *Ostα*$^{-/-}$ mice using a guanodinium thiocyanate/cesium chloride method (Snutch and Mandel 1992). Gene-specific oligonucleotide primers were designed using NCBI Primer-BLAST (Table 1), and samples were analyzed as described above. Fifty ng of total RNA was analyzed per reaction, with the expression of each gene being quantified via a standard curve containing 10-10^{7} copies of the amplicon diluted in yeast total RNA. Expression levels were quantified as a ratio to *Gapdh* levels within each sample and are reported as percent of the values in wild type mice.

Immunohistochemical staining of mouse brain

Male *Ostα*$^{+/+}$ and *Ostα*$^{-/-}$ mice were anesthetized with pentobarbital (50 mg/kg, ip). To fix cerebellar tissue, mice were perfused with 2.5% paraformaldehyde via the heart, and brains were removed and further fixed and cryoprotected by immersion in 1.5% paraformaldehyde and 15% sucrose for 72 h. For hippocampal tissues, mice were perfused with 4% paraformaldehyde, and brains were removed and further fixed by immersion in 4% paraformaldehyde overnight. Brains were then cryoprotected by sequential immersion in 15% and 30% sucrose for 24 h. After freezing the tissues in isopentane (−50°C), they were sectioned using a cryostat into 30 µm sections. Sections from cerebellum and hippocampus were incubated with primary antibodies at 4°C overnight. Antibodies were used at the following dilutions for cerebellum staining: anti-Ostα (mA315) at 1:7200, anti-Ostβ (mB91) at 1:600, IP3R1 (Neuromab) at 1:1000. For hippocampus stainings, antibodies were used at the following dilutions: anti-Ostα (mA315) at 1:4800, anti-Ostβ (mB91) at 1:300, NeuN (Chemicon) at 1:1000. After three washes with TBST, the sections were incubated for 1 h with secondary antibodies (Alexa Fluor 488 1:1000, Alexa Fluor 594 1:1000, both secondary antibodies were obtained from Invitrogen). Slides were mounted using ProLong Gold antifade reagent (Invitrogen) and analyzed using an Olympus FluoView™ FV1000 Laser Scanning Confocal Microscope.

Laser capture microdissection of mouse brain cells

Brains from anesthetized male C57Bl6 mice were snapped frozen in liquid nitrogen, sectioned at 7 µm, and directly collected onto poly-D-lysine coated PEN membrane slides, as previously described (Cui et al. 2009). All solutions were made in DEPC-treated water, and RNAse-Secure (Ambion) was added to the antibody-solutions to remove RNases. Briefly, after blocking for one hour, sections were incubated with primary antibodies for one hour at 37°C, followed by biotinylated secondary antibody for 30 min. Immunoreactivity

was visualized by DAB. Sections were counter-stained with cresyl-violet. At least 500 microdissection captures of each type were made using U-V Laser Microbeam technology (PALM, Carl Zeiss), from each of 4 mice.

DHEA and DHEAS radioimmunoassay

Serum was collected from 7-week old male mice and 9-week old female mice as previously described (Ballatori et al. 2008). All assay components were dissolved in 100 µl of phosphate buffered saline containing 3% w/v bovine serum albumin and 0.01% thimerosal (w/v). The measurement of DHEA employed [^{3}H]DHEA at 0.2 nM and anti-DHEA antibodies (Abcam, Cambridge, MA) at a dilution of 1:50. For serum DHEAS measurements, [^{3}H]DHEAS was used at 0.2 nM and anti-DHEAS antibodies (Genway, San Diego, CA) at a dilution of 1:100. The samples were incubated for 24 h at 4°C. The immunoassays were terminated by addition of 50 µl heat-killed, formalin-fixed 1% (v/v) suspension of *Staphylococcus aureus* cells (Pansorbin®, Calbiochem, USA). The mixtures were incubated for 15–20 min at room temperature and followed with addition of 1ml ice-cold PBS and rapid filtration through glass-fiber filters (GF/C, Whatman, UK) under vacuum. Filter papers were then placed in 3 ml scintillation fluid (Perkin-Elmer, Life and Analytical Sciences) and counted in a Beckman LS 6500 scintillation counter (Beckman Coulter, Fullerton, CA). All measurements were made in duplicate for each sample, and a range of unlabeled standard concentrations were included in each assay for the construction of standard curves. According to the antibody supplier, the anti-DHEA antibody is highly specific to DHEA. The cross reactions with other steroids are: DHEAS 2.6%, androsterone 0.28%, androstenedione 0.17%, 20-dihydroprogesterone 0.02%, 11-hydroxyprogesterone 0.02%, and all other steroids tested less than 0.002%. The anti-DHEAS antibody is also relatively specific to DHEAS: the cross reactivity with DHEA is 25%.

Immunohistochemistry of human tissues

With approval from the University of Rochester's Research Subject Review Board (RSRB) anonymous archival samples from surgical pathology and autopsy pathology research were obtained. Paraffin-embedded human brain and adrenal gland tissues were obtained after all patient identifiers had been removed. Tissue slices of 5 µm were mounted on chemically charged slides, dried at room temperature until opaque and placed in an oven at 57°C overnight. Sections were deparaffinized and quenched with 3% hydrogen peroxide for 6 min. They were then cleared in running water followed by TBS (50 mmol/L Tris-hydrogen chloride, 150 mmol/L sodium chloride, and 0.05% Tween 20 at pH 7.6). Antigen unmasking was performed with preheated (95 to 99°C) citrate buffer, pH 6.1 (DakoCytomation) in a Black and Decker steamer (model HS800; Shelton, CT) for 30 min followed by a 15 min cool down period. Slides were then rinsed with Tris-buffered saline for 5 min and incubated with the primary antibodies human OSTα (hA327; 1:400) or OSTβ (hB1; 1:400) at room temperature for 60 min. The sections were then incubated for 30 min with anti-rabbit antibody labeled with polymer-horseradish peroxidase (Envision Plus System, DakoCytomation). Slides were developed with 3,3'-diaminobenzidine (DAB) (DakoCytomation), rinsed in running distilled water, counterstained in Modified Mayer's Hematoxylin, blued in 0.3% ammonia water followed by a tap water rinse. Slides were mounted using an aqueous media and viewed with a light microscope. Tissue cores with less than 50% of the original tissue left on the slides after immunohistochemistry were not used.

Intraperitoneal administration of [^{3}H]DHEA or [^{3}H]DHEAS to anesthetized mice

Male and female mice that had been fed *ad libitum* were anesthetized by intraperitoneal administration of pentobarbital sodium (50 mg/kg) and additional anesthetic was administered as required for the duration of the experiment. [^{3}H]DHEA or [^{3}H]DHEAS (400 µl of 1 mM; 1 µCi/400 µl) was administered intraperitoneally, and 2 h later whole

blood and tissues were collected. Approximately 0.3 ml of blood was collected from the abdominal aorta in a tared 1ml syringe containing 50 μl of heparin (1000 U/ml). For the liver, approximately 0.2–0.4 g of tissue was taken for analysis of radioisotope content, and the other tissues were collected in their entirety. Tissue and blood samples were placed in tared 20-ml glass vials, and Solvable (Perkin-Elmer, Life and analytical Sciences, Boston, MA) was added to each vial (1.0 ml/0.1 g tissue or 2.0 ml/1.0 ml blood), which was then heated to 60°C for 2 to 3 h. The vials were allowed to cool to room temperature, and 0.1 ml of 0.1 M EDTA/1.0 ml of Solvable was added to each vial of blood. H_2O_2 (30%) was then added in 0.1-ml aliquots (0.3 ml/1.0 ml Solvable for blood or 0.1 ml/1.0 ml Solvable for tissues). After standing at room temperature for 15 to 30 min, the vials were capped tightly and heated to 60°C for 1 h and allowed to cool back to room temperature. After the addition of scintillation fluid (4 ml of Opti-Fluor to 200 μl of each sample) (Perkin-Elmer Life and Analytical Sciences, Boston, MA), the samples were allowed to stand for at least 2 h at room temperature before counting. Samples were counted in a Beckman LS 6500 scintillation counter (Beckman Coulter, Fullerton, CA). Total blood volume was estimated as 6% of body weight.

Statistics

Data are given as means ± SEM. Values were considered to be significantly different, when $p<0.05$ by use of a one-way ANOVA followed by Bonferroni's multiple comparison test or a Student's t-Test where applicable.

Results

[^{3}H]DHEAS and [^{3}H]PREGS are relatively high affinity substrates for OSTα-OSTβ

To characterize the potential substrate specificity of the transporter, initial experiments examined the effects of a variety of conjugated and unconjugated steroids on mouse Ostα–Ostβ or human OSTα–OSTβ-mediated transport of [^{3}H]estrone 3-sulfate in *Xenopus laevis* oocytes (Fig. 1). All of the sulfated and glucuronidated steroids that were examined significantly inhibited transport, whereas the unconjugated parent compounds or compounds without a net negative charge had no effect. Androsterone sulfate and PREGS were the strongest inhibitors of transport, inhibiting transport by about 65% (Fig. 1). Steroid conjugates with more than one sulfate group (estradiol-2S), or with both a sulfate and glucuronic acid moiety (estradiol-S-G) also inhibited transport activity (Fig. 1). The inhibition by the conjugated steroids suggests but does not establish that they are substrates for this carrier.

To directly test whether DHEA, DHEAS, PREG, and PREGS are substrates for the transporter, uptake of these radiolabeled compounds was measured in *Xenopus* oocytes expressing human OSTα–OSTβ. [^{3}H]DHEAS uptake was markedly higher in OSTα–OSTβ-expressing oocytes (Fig. 2A), confirming previous findings (Ballatori et al. 2005). [^{3}H]PREGS uptake was also higher in OSTα–OSTβ-expressing oocytes (Fig. 2B), whereas there was no significant difference in [^{3}H]DHEA and [^{3}H]PREG uptake between control and OSTα–OSTβ-expressing oocytes (Fig. 2A and B).

To establish the kinetics of [^{3}H]DHEAS and [^{3}H]PREGS transport, initial rates of uptake of these compounds (5 min) was measured over a concentration range of 0.1–800 μM (Figs. 2C and D). Eadie-Hofstee plots for DHEAS and PREGS suggested two transport components for each compound. The Km values for the high affinity transport components were 1.5±0.4 μM for DHEAS and 6.9±2.1 μM for PREGS, whereas the low affinity components gave Km values of 532±58 and 909±72 μM for DHEAS and PREGS, respectively. The high-affinity Km value for DHEAS is within the physiological plasma concentration range for this steroid

in humans (1–5 μM; Dharia and Parker 2004), whereas the high-affinity Km value of PREGS is higher than plasma PREGS concentration (11–15 nM; Wang et al. 1996). However, because OSTα–OSTβ is expected to mediate primarily sterol export from cells, the intracellular concentration is the more meaningful parameter in defining the kinetics, but unfortunately intracellular concentrations of sterols are largely unknown and difficult to assess.

*OST*α and *OST*β mRNA is expressed in human and mouse brain, and in steroidogenic tissues

*OST*α and *OST*β mRNA was detected in all major human steroidogenic tissues, namely the testis, ovary, adrenal gland and prostate (Fig. 3A), in agreement with previous findings (Seward et al. 2003). Interestingly, although overall human brain *OST*α and *OST*β mRNA levels are relatively low (Seward et al. 2003), relatively high levels of *OST*α and *OST*β mRNA were found in the hippocampus (Fig. 3B). *OST*β mRNA was also detected in the cerebellum, but *OST*α was below the limit of detection in this brain region (Fig. 3B).

Analysis of mouse brain and steroidogenic tissues revealed that *Ost*α and *Ost*β mRNA levels appeared to be much lower than those in human tissues, and were below the detection limit in mouse cerebellum and hippocampus (Fig. 3C); however, a direct quantitative comparison of relative abundance between mouse and human is not possible from the present data given that different primer sets were used. Although *Ost*α and *Ost*β mRNA levels were below the detection limit in the mouse cerebellum and hippocampus, when specific mouse brain cells were isolated using laser capture microdissection, *Ost*α and *Ost*β mRNA was detected in Purkinje cells and cells in the CA region of the hippocampus (Fig. 3D). Inositol 1,4,5-trisphosphate receptor type 1 (IP3R1) was used as a marker for Purkinje cells and the hippocampal neurons (Fig. 3E). IP3R1 is a key neuronal IP3R in the central nervous system: it is predominantly concentrated in Purkinje cells and the CA1 region of hippocampus, with low expression in granular cells of the cerebellum (Aoki et al. 2003;Choi et al. 2004;Hisatsune et al. 2006).

Human OSTα and OSTβ and mouse Ostα and Ostβ proteins are selectively localized to steroidogenic cells in the brain

Antibodies to Ostα and Ostβ localized these proteins to specific cells within the cerebellar cortex and hippocampus of wild type male mice, whereas relatively little staining was noted in *Ost*α-deficient mice (Fig. 4). As previously reported, Ostα-deficient mice lack Ostα protein and have very low Ostβ protein expression (Li et al. 2007). In the cerebellar cortex, intense immunoreactivity was noted in large cell bodies lying at a narrow zone between the granular and molecular layers, which is coincident with the location of Purkinje cells (Fig. 4, A1–A6 and B1–B6). Ostα and Ostβ proteins co-localized with the IP3R1 protein, which is a Purkinje cell marker. In the hippocampus, these proteins appeared to be localized to the neurons of CA1, CA2, CA3, and dentate gyrus regions (Fig. 4, D1–D6 and E1–E6). These are the same regions that have previously been shown to express steroidogenic enzymes (Mellon and Deschepper 1993;Kimoto et al. 2001;Ukena et al. 1998;Zwain and Yen 1999). In the human brain, antibodies to OSTα and OSTβ localized these proteins to similar regions as in the mouse brain (Fig. 5A–L).

OSTα and OSTβ proteins are most abundant in the *zona reticularis* of the human adrenal gland

In the human adrenal gland, OSTα and OSTβ immunoreactivity was noted largely in the *zona reticularis* (Fig. 5M–P), the region that is primarily responsible for the secretion of DHEAS from the adrenal gland (Rainey et al. 2002). Staining was weak in the *zona*

glomerulosa and *zona fasciculata* (Fig. 5M and O). At higher magnification (Fig. 5N and P), staining was clearly noted in cells within these regions.

Serum DHEA and DHEAS levels are altered in *Ostα*$^{-/-}$ mice

As an indirect test of the hypothesis that Ostα-Ostβ contributes to neurosteroid disposition, serum levels of DHEA and DHEAS were measured in *Ostα*$^{+/+}$ and *Ostα*$^{-/-}$ mice (Fig. 6). Serum DHEA levels were higher in both male and female *Ostα*$^{-/-}$ mice (8% in male, 12% in female), whereas serum DHEAS levels were lower (16% in male, 18% in female), such that the DHEA/DHEAS ratio was substantially higher in *Ostα*$^{-/-}$ mice (Fig. 6C).

Altered tissue distribution of [^{3}H]DHEAS in *Ostα*$^{-/-}$ mice

To further characterize the role of Ostα-Ostβ in the *in vivo* disposition of DHEA or DHEAS, the tissue distribution of [^{3}H]DHEA and [^{3}H]DHEAS was measured at 2 h after their intraperitoneal administration in *Ostα*-deficient and wild type mice (Fig. 7). For DHEA there were no significant differences in tissue distribution of radioactivity between *Ostα*-deficient and wild type mice (data not shown), whereas tissue [^{3}H]DHEAS distribution was different (Fig. 7). In particular, note that more radioactivity was found in the liver and adrenal gland of both male and female *Ostα*$^{-/-}$ mice, although these differences were statistically significant only in the male mice (Fig. 7).

To identify possible mechanisms for the changes in serum DHEA/DHEAS levels in the *Ostα*-deficient mice, the expression of some of the key genes involved in their homeostasis were measured in liver. In rodents, DHEA and DHEAS are synthesized mainly in the liver and gonads (Brock and Waterman 1999; Katagiri et al. 1998; Kobayashi et al. 2003). Although expression of Ostα-Ostβ is low in the whole mouse liver, these proteins may nevertheless contribute to hepatobiliary disposition of bile acids and related molecules in the mouse (Ballatori et al. 2005). As previously reported (Ballatori et al., 2008; Rao et al. 2008), hepatic expression of *Cyp7a1*, a key enzyme in the conversion of cholesterol to bile acids was markedly reduced in *Ostα*-deficient mice (Fig. 8); however, there were no major changes in the expression of some of the key genes involved in steroid biosynthesis, including *Cyp11a1*, *Cyp17a1*, and *Sul2a1*, indicating that the altered serum DHEA and DHEAS levels in the *Ostα*-deficient mice cannot be readily explained by changes in the expression of these steroid biosynthesis genes.

Discussion

The present results provide support for the hypothesis that OSTα–OSTβ contributes the transport of conjugated steroids in steroidogenic cells by demonstrating that OSTα and OSTβ are expressed in the specific brain and adrenal gland cells that are involved in steroidogenesis, that PREGS and DHEAS, two important steroid hormone precursors in the periphery and potent neurosteroids in the central nervous system, are relatively high-affinity substrates for OSTα–OSTβ, and that *Ostα*-deficient mice exhibit altered serum DHEA and DHEAS levels, and [^{3}H]DHEAS distribution.

OSTα-OSTβ is a recently identified organic solute and steroid carrier that plays a central role in the transport of bile acids in the intestine, liver, and kidney, and in regulating the enterohepatic circulation (Ballatori et al. 2009). Mice that are deficient in *Ostα* exhibit a defect in intestinal bile acid absorption, a markedly diminished bile acid pool size, intestinal hypertrophy, growth retardation, a decrease in serum cholesterol and triglyceride levels, and an increase in fecal excretion of neutral sterols (Ballatori et al. 2008; Rao et al. 2008). Although these previous studies indicate that Ostα-Ostβ is critical for bile acid homeostasis, they also demonstrate that alternate or compensatory mechanisms are present in the Ostα$^{-/-}$

mice that allow bile acids to still be absorbed, albeit less efficiently than in wild type animals (Ballatori et al. 2008; Rao et al. 2008).

Because of the major role of OSTα-OSTβ in bile acid homeostasis, most studies to date have focused on its functions in the gastrointestinal tract (Ballatori et al. 2005, 2008, 2009; Rao et al. 2008). However, OSTα and OSTβ are also expressed in many tissues that do not normally handle bile acids (Seward et al. 2003), indicating that these proteins are likely serving some other roles in these tissues. In particular, *OST*α and *OST*β mRNA is also expressed in the brain, the adrenal gland, and all major steroidogenic tissues (Seward et al. 2003; and Fig. 3), suggesting a potential role in steroid transport in these tissues. The present findings provide support for this hypothesis.

The present results also provide additional insight into the substrate specificity of OSTα-OSTβ. Previous studies demonstrated that a number of bile acids are substrates, and that sulfated bile salts are among the powerful inhibitors of transport (Ballatori et al. 2005; Seward et al. 2003; Wang et al. 2001). The present results demonstrate that sulfated steroids exhibit the strongest inhibitory effect on both mouse Ostα-Ostβ and human OSTα-OSTβ mediated estrone 3-sulfate transport (Fig. 1A, B). Glucuronidated steroids also inhibited transport, although they appeared to be weaker inhibitors. In contrast, the parent steroids and exogenous steroid conjugates with no net charge showed no significant inhibition of OSTα-OSTβ mediated transport, indicating that charge distribution and molecular structure of the molecule may determine its affinity for OSTα-OSTβ.

By direct measurement of transport, the present results also demonstrate that PREGS and DHEAS are substrates for OSTα-OSTβ, but that the parent compounds (PREG and DHEA) do not appear to be substrates. The kinetics of OSTα-OSTβ mediated DHEAS and PREGS transport indicate both high-affinity and low-affinity components for these compounds. The apparent Km value for the high affinity component of DHEAS transport was 1.5±0.4 μM, which is within the range of human blood plasma DHEAS levels (1–5 μM). Plasma levels of PREGS are generally in the nM range, but nanomolar to micromolar concentrations of PREGS have been shown to alter presynaptic or postsynaptic actions in the brain (Gibbs et al. 2006; Meyer et al. 2002; Monnet et al. 1995), and thus the high-affinity component of PREGS transport (apparent Km of 6.9±2.1 μM) may also be physiologically relevant. However, as noted earlier, because OSTα–OSTβ is expected to mediate primarily sterol export from cells, the intracellular concentration is the more meaningful parameter in defining the kinetics, but unfortunately intracellular concentrations of sterols are difficult to assess.

Our observation that OSTα-OSTβ exhibits both low- and high-affinity transport components also provides insight into the molecular mechanisms of transport. Multiple transport components transport may occur when a transporter has more than one substrate binding sites, or when the transporter has a substrate binding site that assumes different conformations depending, for example, on the type and extent of post-translational modifications or on the presence of accessory proteins or other factors (Eisenhaber and Eisenhaber 2007; Malo and Fliegel 2006; Putman et al. 2000; Sauna et al. 2001; van den Berghe and Klomp 2010; van der Heide and Poolman 2002). Additional studies are needed to define whether OSTα-OSTβ contains more than one substrate binding site or whether it exists in different conformations, and to define the physiological relevance of the low affinity transport component.

In addition to OSTα-OSTβ substrate specificity and transport kinetics, the selective localization of these proteins to steroidogenic cells in the brain and adrenal gland provides additional evidence for the hypothesis that OSTα-OSTβ contributes to the disposition of

sulfated steroids in these tissues. Previous studies have demonstrated that both the mouse and human brain contain the enzymes needed for synthesizing DHEAS and PREGS, including the steroid sulfotransferase SULT2A1/Sult2a1 (Kimoto et al. 2001; Maninger et al. 2009; Mellon and Deschepper 1993; Ukena et al. 1998; Zwain and Yen 1999). In particular, Purkinje cells and hippocampal neurons have been shown to possess steroidogenic enzymes and to produce DHEA, PREG and their sulfated esters. Both of these brain regions are well known for their function in the process of learning and memory, and several studies have suggested that the hippocampus is a site for PREGS action (Akwa et al. 2001; Flood et al. 1995). The present results demonstrate these same brain regions are recognized by the OSTα/Ostα and OSTβ/Ostβ antibodies in both human and mouse brain, indicating co-localization of the transporter with the steroid biosynthetic enzymes.

Interestingly, in a recent study designed to gain insight into the function of proteins involved in Purkinje cells degeneration, Lim and coworkers (2006) used a yeast two-hybrid screen to identify OSTα as one of the proteins that can interact with ataxin-1, a polyglutamine protein of unknown function, whose mutant form causes type 1 spinocerebellar ataxia (SCA1) in humans. Cerebellar Purkinje cells appear to be the major cell type affected in this inherited neurodegenerative disease, and targeted expression of mutant ataxin-1 in Purkinje cells of transgenic mice produces an ataxic phenotype with pathological similarities to the human disease (Clark and Orr 2000). The significance of the ataxin-1-OSTα protein-protein interaction is presently unknown, but it does provide clues into both the function of ataxin-1 and into the pathogenesis of SCA1.

Although mouse and human brain are both capable of synthesizing DHEA and DHEAS, mice and humans differ markedly in the major site of DHEA and DHEAS synthesis in the periphery and in concentrations of these steroids in blood. In humans, the adrenal gland cells within the *zona reticularis* of the cortex serve as the major site of synthesis of circulating DHEA and DHEAS, and serum concentrations of these steroids are quite high, 1–5 μM (Rainey et al. 2002; Rainey and Nakamura 2008). In contrast, in the mouse, DHEA and DHEAS are synthesized mainly in the gonads and liver, and mouse blood concentrations are much lower than in humans, 0.01–0.05 μM (Brock and Waterman 1999; Katagiri et al. 1998; Kobayashi et al. 2003). The present results demonstrate that the *zona reticularis* of the human adrenal gland cortex is relatively selectively stained by the OSTα and OSTβ antibodies, whereas the expression of *Ostα* and *Ostβ* mRNA in mouse adrenal gland was quite low and Ostα and Ostβ proteins could not be detected in this tissue. Thus, both the strong expression of OSTα-OSTβ in human adrenal gland cells that synthesize DHEA and DHEAS, and conversely, the low expression of these synthetic and putative transport genes in the mouse adrenal gland, are consistent with the hypothesis that this transporter is involved in DHEAS disposition.

It is now well established that *Ostα* and *Ostβ* mRNA expression is regulated by bile acids via the farnesoid X receptor (FXR; Boyer et al. 2006; Frankenberg et al. 2006; Landrier et al. 2006; Lee et al. 2006). Interestingly, *CYP17* and dehydroepiandrosterone sulfotransferase *Sult2a1*, which encode for two key enzymes for DHEAS production, are also positively regulated by FXR (Song et al. 2001). These similar regulatory mechanisms further support the hypothesis that Ostα-Ostβ is responsible for transporting DHEAS. Given that this transporter is also expressed in other steroidogenic tissues, it will be interesting to examine the localization and function of Ostα-Ostβ in these tissues. In particular, previous studies have demonstrated that estrone 3-sulfate and DHEAS, known substrates for Ostα-Ostβ, can be taken up by the testis, ovary, and mammary gland and converted back to active steroid hormones within these tissues, and it is tempting to speculate that Ostα-Ostβ may be involved in these processes. Steroid uptake by these tissues has also been associated with the induction and maintenance of endocrine-dependent cancers, namely prostate cancer and

breast cancer (Billich et al. 2000; Falany and Falany 1997; Purohit et al. 1999), and it will be of interest to examine whether this transporter may be involved.

Of significance, although direct quantitative comparisons of mRNA levels between human and mouse tissues are not possible from the present data, *OST*α and *OST*β mRNA expression in human brain and steroidogenic tissues appears to be much higher than that in the corresponding mouse tissues (Fig. 3), and these species differences parallel the differences in serum DHEAS levels. As noted above, human serum DHEAS concentrations are in the range of 1–5 μM (Dharia and Parker 2004;Rainey and Nakamura 2008), whereas mouse serum DHEAS levels are about 2 orders of magnitude lower, or 0.01–0.05 μM (Kobayashi et al. 2003; and Fig. 6). In *Ostα*$^{-/-}$ mice, serum DHEA and DHEAS levels and the distribution of administered [^{3}H]DHEAS were altered, providing indirect evidence for a role of the transporter in neurosteroid disposition.

Although the mechanism for the altered DHEA/DHEAS levels in *Ostα*$^{-/-}$ mice is presently undefined, some factors that may be involved include: a) diminished efflux of DHEAS from steroidogenic cells, as supported by the present findings showing that DHEAS is a relatively high affinity substrate for Ostα-Ostβ and that this transporter is localized to these cells; b) impaired biosynthesis of DHEA due to an imbalance of cholesterol and bile acid homeostasis, as previously reported in *Ostα*$^{-/-}$ mice (Ballatori et al. 2008; Rao et al. 2008); c) decreased elimination of DHEA from the serum compartment; or d) decreased activity of the enzyme(s) that convert DHEA to DHEAS. However, the present findings demonstrate that hepatic expression of *Sult2a1*, an important enzyme for the conversion of DHEA to DHEAS, was similar in both genotypes.

In summary, the present findings demonstrate that OSTα and OSTβ are expressed in steroidogenic cells in the brain and adrenal gland, and that this transporter can transport DHEAS and PREGS with high affinity. Thus, OSTα-OSTβ may contribute to neurosteroid transport in the brain and sterol conjugate transport in the adrenal gland and other steroidogenic tissues.

Abbreviations used

CA	*cornu ammonis*
DBA	3,3’-diaminobenzidine
DHEA	dehydroepiandrosterone
DHEAS	dehydroepiandrosterone sulfate
estradiol-2S	β-estradiol 3,17-disulfate
estradiol-S-G	β-estradiol 3-(β-D-glucuronide) 17-sulfate
OST/Ost	organic solute transporter
PREG	pregnenolone
PREGS	pregnenolone sulfate

Acknowledgments

This work was supported in part by National Institute of Health Grant DK067214 (NB), ES014899 and ES17470 (KT), American Cancer Society RSG-07-092-01-TBE (JH), and National Institute of Environmental Health Sciences Training Grant ES07026 and Center Grant ES01247 (NB).

We thank Qi Yang, Patricia Bourne, and Drs. Christine Hammond and Jeorge Yao for their assistance with some of the analyses, and Dr. Berislav Zlokovic for access to the laser capture microdissection instrumentation. The

monoclonal antibody mouse anti-IP3R1 was obtained from the UC Davis/NIH NeuroMab Facility, supported by NIH grant U24NS050606 and maintained by the Department of Neurobiology, Physiology and Behavior, College of Biological Sciences, University of California, Davis, CA 95616.

References

Akwa Y, Ladurelle N, Covey DF, Baulieu EE. The synthetic enantiomer of pregnenolone sulfate is very active on memory in rats and mice, even more so than its physiological neurosteroid counterpart: distinct mechanisms? Proc. Natl. Acad. Sci. USA. 2001; 98:14033–14037. [PubMed: 11717462]

Aoki T, Narita M, Ohnishi O, Mizuo K, Narita M, Yajima Y, Suzuki T. Disruption of the type 1 inositol 1,4,5-trisphosphate receptor gene suppresses the morphine-induced antinociception in the mouse. Neurosci.. Lett. 2003; 350:69–72. [PubMed: 12972155]

Asif AR, Steffgen J, Metten M, Grunewald RW, Müller GA, Bahn A, Burckhardt G, Hagos Y. Presence of organic anion transporters 3 (OAT3) and 4 (OAT4) in human adrenocortical cells. Pflugers Arch. 2005; 450:88–95. [PubMed: 15864504]

Ballatori N, Christian WV, Lee JY, Dawson PA, Soroka CJ, Boyer JL, Madejczyk MS, Li N. OSTα-OSTβ: a major basolateral bile acid and steroid transporter in human intestinal, renal, and biliary epithelia. Hepatology. 2005; 42:1270–1279. [PubMed: 16317684]

Ballatori N, Fang F, Christian WV, Li N, Hammond CL. Ostα-Ostβ is required for bile acid and conjugated steroid disposition in the intestine, kidney, and liver. Am. J. Physiol. Gastrointest. Liver Physiol. 2008; 295:G179–G186. [PubMed: 18497332]

Ballatori N, Li N, Fang F, Boyer JL, Christian WV, Hammond CL. OSTα-OSTβ: a key membrane transporter of bile acids and conjugated steroids. Frontiers in Bioscience. 2009; 14:2829–2844. [PubMed: 19273238]

Bortfeld M, Rius M, König J, Herold-Mende C, Nies AT, Keppler D. Human multidrug resistance protein 8 (MRP8/ABCC11), an apical efflux pump for steroid sulfates, is an axonal protein of the CNS and peripheral nervous system. Neuroscience. 2006; 137:1247–1257. [PubMed: 16359813]

Billich A, Nussbaumer P, Lehr P. Stimulation of MCF-7 breast cancer cell proliferation by estrone sulfate and dehydroepiandrosterone sulfate: inhibition by novel non-steroidal steroid sulfatase inhibitors. J. Steroid Biochem. Mol. Biol. 2000; 73:225–235. [PubMed: 11070351]

Boyer JL, Trauner M, Mennone A, Soroka CJ, Cai SY, Moustafa T, Zollner G, Lee JY, Ballatori N. Upregulation of a basolateral FXR-dependent bile acid efflux transporter OSTalpha-OSTbeta in cholestasis in humans and rodents. Am. J. Physiol. Gastrointest. Liver Physiol. 2006; 290:G1124–G1130. [PubMed: 16423920]

Brock BJ, Waterman MR. Biochemical differences between rat and human cytochrome P450c17 support the different steroidogenic needs of these two species. Biochemistry. 1999; 38:1598–1606. [PubMed: 9931027]

Chen ZS, Guo Y, Belinsky MG, Kotova E, Kruh GD. Transport of bile acids, sulfated steroids, estradiol 17-beta-D-glucuronide, and leukotriene C4 by human multidrug resistance protein 8 (ABCC11). Mol. Pharmacol. 2005; 67:545–557. [PubMed: 15537867]

Choi JY, Beaman-Hall CM, Vallano ML. Granule neurons in cerebellum express distinct splice variants of the inositol trisphosphate receptor that are modulated by calcium. Am. J. Physiol. Cell Physiol. 2004; 287:C971–C980. [PubMed: 15189817]

Clark HB, Orr HT. Spinocerebellar ataxia type 1--modeling the pathogenesis of a polyglutamine neurodegenerative disorder in transgenic mice. J. Neuropathol. Exp. Neurol. 2000; 59:265–270. [PubMed: 10759181]

Corpéchot C, Robel P, Axelson M, Sjovall J, Baulieu EE. Characterization and measurement of dehydroepiandrosterone sulfate in rat brain. Proc. Natl. Acad. Sci. USA. 1981; 78:4704–4707. [PubMed: 6458035]

Corpéchot C, Synguelakis M, Talha S, Axelson M, Sjövall J, Vihko R, Baulieu EE, Robel P. Pregnenolone and its sulfate ester in the rat brain. Brain Res. 1983; 270:119–125. [PubMed: 6223687]

Cui M, Aras R, Christian WV, Rappold PM, Hatwar M, Panza J, Jackson-Lewis V, Javitch JA, Ballatori N, Przedborski S, Tieu K. The organic cation transporter-3 is a pivotal modulator of

neurodegeneration in the nigrostriatal dopaminergic pathway. Proc. Natl. Acad. Sci. USA. 2009; 106:8043–8048. [PubMed: 19416912]

Dawson PA, Hubbert M, Haywood J, Craddock AL, Zerangue N, Christian WV, Ballatori N. The heteromeric organic solute transporter alpha-beta, Ostalpha-Ostbeta, is an ileal basolateral bile acid transporter. J. Biol. Chem. 2005; 280:6960–6968. [PubMed: 15563450]

Dharia S, Parker CR Jr. Adrenal androgens and aging. Semin. Reprod. Med. 2004; 22:361–368. [PubMed: 15635503]

Do Rego JL, Seong JY, Burel D, Leprince J, Luu-The V, Tsutsui K, Tonon MC, Pelletier G, Vaudry H. Neurosteroid biosynthesis: enzymatic pathways and neuroendocrine regulation by neurotransmitters and neuropeptides. Front. Neuroendocrinol. 2009; 30:259–301. [PubMed: 19505496]

Eisenhaber B, Eisenhaber F. Posttranslational modifications and subcellular localization signals: indicators of sequence regions without inherent 3D structure? Curr. Protein Pept. Sci. 2007; 8:197–203. [PubMed: 17430201]

Eser D, Schüle C, Baghai TC, Romeo E, Rupprecht R. Neuroactive steroids in depression and anxiety disorders: clinical studies. Neuroendocrinology. 2006; 84:244–254. [PubMed: 17159334]

Falany JL, Falany CN. Regulation of estrogen activity by sulfation in human MCF-7 breast cancer cells. Oncol. Res. 1997; 9:589–596. [PubMed: 9563006]

Flood JF, Roberts E. Dehydroepiandrosterone sulfate improves memory in aging mice. Brain Res. 1988; 448:178–181. [PubMed: 2968829]

Flood JF, Morley JE, Roberts E. Pregnenolone sulfate enhances post-training memory processes when injected in very low doses into limbic system structures: the amygdala is by far the most sensitive. Proc. Natl. Acad. Sci. USA. 1995; 92:10806–10810. [PubMed: 7479888]

Frankenberg T, Rao A, Chen F, Haywood J, Shneider BL, Dawson PA. Regulation of the mouse organic solute transporter alpha-beta, Ostalpha-Ostbeta, by bile acids. Am. J. Physiol. Gastrointest. Liver Physiol. 2006; 290:G912–G922. [PubMed: 16357058]

Gibbs TT, Russek SJ, Farb DH. Sulfated steroids as endogenous neuromodulators. Pharmacol. Biochem. Behav. 2006; 84:555–567. [PubMed: 17023038]

Goldin AL. Maintenance of *Xenopus laevis* and oocyte injection. Methods Enzymol. 1992; 207:266–279. [PubMed: 1528120]

Hisatsune C, Kuroda Y, Akagi T, Torashima T, Hirai H, Hashikawa T, Inoue T, Mikoshiba K. Inositol 1,4,5-trisphosphate receptor type 1 in granule cells, not in Purkinje cells, regulates the dendritic morphology of Purkinje cells through brain-derived neurotrophic factor production. J. Neurosci. 2006; 26:10916–10924. [PubMed: 17050730]

Isaacson RL, Varner JA, Baars JM, De Wied D. The effects of pregnenolone sulfate and ethylestrenol on retention of a passive avoidance task. Brain Res. 1995; 689:79–84. [PubMed: 8528708]

Katagiri M, Tatsuta K, Imaoka S, Funae Y, Honma K, Matsuo N, Yokoi H, Ishimura K, Ishibashi F, Kagawa N. Evidence that immature rat liver is capable of participating in steroidogenesis by expressing 17alpha-hydroxylase/17,20-lyase P450c17. J. Steroid Biochem. Mol. Biol. 1998; 64:121–128. [PubMed: 9569017]

Kimoto T, Tsurugizawa T, Ohta Y, Makino J, Tamura H, Hojo Y, Takata N, Kawato S. Neurosteroid synthesis by cytochrome p450-containing systems localized in the rat brain hippocampal neurons: N-methyl-D-aspartate and calcium-dependent synthesis. Endocrinology. 2001; 142:3578–3589. [PubMed: 11459806]

Kobayashi Y, Tagawa N, Muraoka K, Okamoto Y, Nishida M. Participation of endogenous dehydroepiandrosterone and its sulfate in the pathology of collagen-induced arthritis in mice. Biol. Pharm. Bull. 2003; 26:1596–1599. [PubMed: 14600408]

Landrier JF, Eloranta JJ, Vavricka SR, Kullak-Ublick GA. The nuclear receptor for bile acids, FXR, transactivates human organic solute transporter-alpha and -beta genes. Am. J. Physiol. Gastrointest. Liver Physiol. 2006; 290:G476–G485. [PubMed: 16269519]

Lee H, Zhang Y, Lee FY, Nelson SF, Gonzalez FJ, Edwards PA. FXR regulates organic solute transporters alpha and beta in the adrenal gland, kidney, and intestine. J. Lipid Res. 2006; 47:201–214. [PubMed: 16251721]

Li N, Cui Z, Fang F, Lee JY, Ballatori N. Heterodimerization, trafficking and membrane topology of the two proteins, Ost alpha and Ost beta, that constitute the organic solute and steroid transporter. Biochem. J. 2007; 407:363–372. [PubMed: 17650074]

Lim J, Hao T, Shaw C, Patel AJ, Szabó G, Rual JF, Fisk CJ, Li N, Smolyar A, Hill DE, Barabási AL, Vidal M, Zoghbi HY. A protein-protein interaction network for human inherited ataxias and disorders of Purkinje cell degeneration. Cell. 2006; 125:801–814. [PubMed: 16713569]

Majewska MD, Demirgoren S, Spivak CE, London ED. The neurosteroid dehydroepiandrosterone sulfate is an allosteric antagonist of the GABAA receptor. Brain Res. 1990; 526:143–146. [PubMed: 1964106]

Malo ME, Fliegel L. Physiological role and regulation of the Na+/H+ exchanger. Can. J. Physiol. Pharmacol. 2006; 84:1081–1095. [PubMed: 17218973]

Maninger N, Wolkowitz OM, Reus VI, Epel ES, Mellon SH. Neurobiological and neuropsychiatric effects of dehydroepiandrosterone (DHEA) and DHEA sulfate (DHEAS). Front. Neuroendocrinol. 2009; 30:65–91. [PubMed: 19063914]

Mellon SH. Neurosteroid regulation of central nervous system development. Pharmacol. Ther. 2007; 116:107–124. [PubMed: 17651807]

Mellon SH, Deschepper CF. Neurosteroid biosynthesis: genes for adrenal steroidogenic enzymes are expressed in the brain. Brain Res. 1993; 629:283–292. [PubMed: 8111631]

Mellon SH, Griffin LD, Compagnone NA. Biosynthesis and action of neurosteroids. Brain Res. Rev. 2001; 37:3–12. [PubMed: 11744070]

Meyer DA, Carta M, Partridge LD, Covey DF, Valenzuela CF. Neurosteroids enhance spontaneous glutamate release in hippocampal neurons. Possible role of metabotropic sigma1-like receptors. J. Biol. Chem. 2002; 277:28725–28732. [PubMed: 12042305]

Monnet FP, Mahé V, Robel P, Baulieu EE. Neurosteroids, via sigma receptors, modulate the [3H]norepinephrine release evoked by N-methyl-D-aspartate in the rat hippocampus. Proc. Natl. Acad. Sci. USA. 1995; 92:3774–3778. [PubMed: 7731982]

Nozaki Y, Kusuhara H, Kondo T, Hasegawa M, Shiroyanagi Y, Nakazawa H, Okano T, Sugiyama Y. Characterization of the uptake of organic anion transporter (OAT) 1 and OAT3 substrates by human kidney slices. J. Pharmacol. Exp. Ther. 2007; 321:362–369. [PubMed: 17255469]

Park-Chung M, Wu FS, Purdy RH, Malayev AA, Gibbs TT, Farb DH. Distinct sites for inverse modulation of N-methyl-D-aspartate receptors by sulfated steroids. Mol. Pharmacol. 1997; 52:1113–1123. [PubMed: 9396781]

Pizzagalli F, Varga Z, Huber RD, Folkers G, Meier PJ, St-Pierre MV. Identification of steroid sulfate transport processes in the human mammary gland. J. Clin. Endocrinol. Metab. 2003; 88:3902–3912. [PubMed: 12915686]

Purohit A, Singh A, Reed MJ. Regulation of steroid sulphatase and oestradiol 17β-hydroxysteroid dehydrogenase in breast cancer. Biochem. Soc. Trans. 1999; 27:323–327. [PubMed: 10093756]

Putman M, van Veen HW, Konings WN. Molecular properties of bacterial multidrug transporters. Microbiol. Mol. Biol. Rev. 2000; 64:672–693. [PubMed: 11104814]

Rainey WE, Carr BR, Sasano H, Suzuki T, Mason JI. Dissecting human adrenal androgen production. Trends Endocrinol. Metab. 2002; 13:234–239. [PubMed: 12128283]

Rainey WE, Nakamura Y. Regulation of the adrenal androgen biosynthesis. J. Steroid Biochem. Mo.l Biol. 2008; 108:281–286.

Rao A, Haywood J, Craddock AL, Belinsky MG, Kruh GD, Dawson PA. The organic solute transporter alpha-beta, Ostalpha-Ostbeta, is essential for intestinal bile acid transport and homeostasis. Proc. Natl. Acad. Sci. USA. 2008; 105:3891–3896. [PubMed: 18292224]

Sauna ZE, Smith MM, Müller M, Kerr KM, Ambudkar SV. The mechanism of action of multidrug-resistance-linked P-glycoprotein. J. Bioenerg. Biomembr. 2001; 33:481–491. [PubMed: 11804190]

Schumacher M, Liere P, Akwa Y, Rajkowski K, Griffiths W, Bodin K, Sjövall J, Baulieu EE. Pregnenolone sulfate in the brain: A controversial neurosteroid. Neurochem. Int. 2008; 52:522–540. [PubMed: 18068870]

Seward DJ, Koh AS, Boyer JL, Ballatori N. Functional complementation between a novel mammalian polygenic transport complex and an evolutionarily ancient organic solute transporter, OSTalpha-OSTbeta. J. Biol. Chem. 2003; 278:27473–27482. [PubMed: 12719432]

Snutch TP, Mandel G. Tissue RNA as source of ion channels and receptors. Methods in Enzymology. 1992; 207:297–309. [PubMed: 1382185]

Song CS, Echchgadda I, Baek BS, Ahn SC, Oh T, Roy AK, Chatterjee B. Dehydroepiandrosterone sulfotransferase gene induction by bile acid activated farnesoid X receptor. J. Biol. Chem. 2001; 276:42549–42556. [PubMed: 11533040]

Stoffel-Wagner B. Neurosteroid biosynthesis in the human brain and its clinical implications. Ann. N.Y. Acad. Sci. 2003; 1007:64–78. [PubMed: 14993041]

Suzuki M, Suzuki H, Sugimoto Y, Sugiyama Y. ABCG2 transports sulfated conjugates of steroids and xenobiotics. J. Biol. Chem. 2003; 278:22644–22649. [PubMed: 12682043]

Tsutsui K. Neurosteroids in the Purkinje cell: biosynthesis, mode of action and functional significance. Mol. Neurobiol. 2008; 37:116–125. [PubMed: 18521763]

Ukena K, Usui M, Kohchi C, Tsutsui K. Cytochrome P450 side-chain cleavage enzyme in the cerebellar Purkinje neuron and its neonatal change in rats. Endocrinology. 1998; 139:137–147. [PubMed: 9421408]

Wang M, Seippel L, Purdy RH, Bãckström T. Relationship between symptom severity and steroid variation in women with premenstrual syndrome: study on serum pregnenolone, pregnenolone sulfate, 5 alpha-pregnane-3,20-dione and 3 alpha-hydroxy-5 alpha-pregnan-20-one. J. Clin. Endocrinol. Metab. 1996; 81:1076–1082. [PubMed: 8772579]

Wang W, Seward DJ, Li L, Boyer JL, Ballatori N. Expression cloning of two genes that together mediate organic solute and steroid transport in the liver of a marine vertebrate. Proc. Natl. Acad. Sci. USA. 2001; 98:9431–9436. [PubMed: 11470901]

van den Berghe PV, Klomp LW. Posttranslational regulation of copper transporters. J. Biol. Inorg. Chem. 2010; 15:37–46. [PubMed: 19813030]

van der Heide T, Poolman B. ABC transporters: one, two or four extracytoplasmic substrate-binding sites? EMBO Rep. 2002; 3:938–943. [PubMed: 12370206]

Zelcer N, Reid G, Wielinga P, Kuil A, van der Heijden I, Schuetz JD, Borst P. Steroid and bile acid conjugates are substrates of human multidrug-resistance protein (MRP) 4 (ATP-binding cassette C4). Biochem. J. 2003; 371:361–367. [PubMed: 12523936]

Zwain IH, Yen SS. Neurosteroidogenesis in astrocytes, oligodendrocytes, and neurons of cerebral cortex of rat brain. Endocrinology. 1999; 140:3843–3852. [PubMed: 10433246]

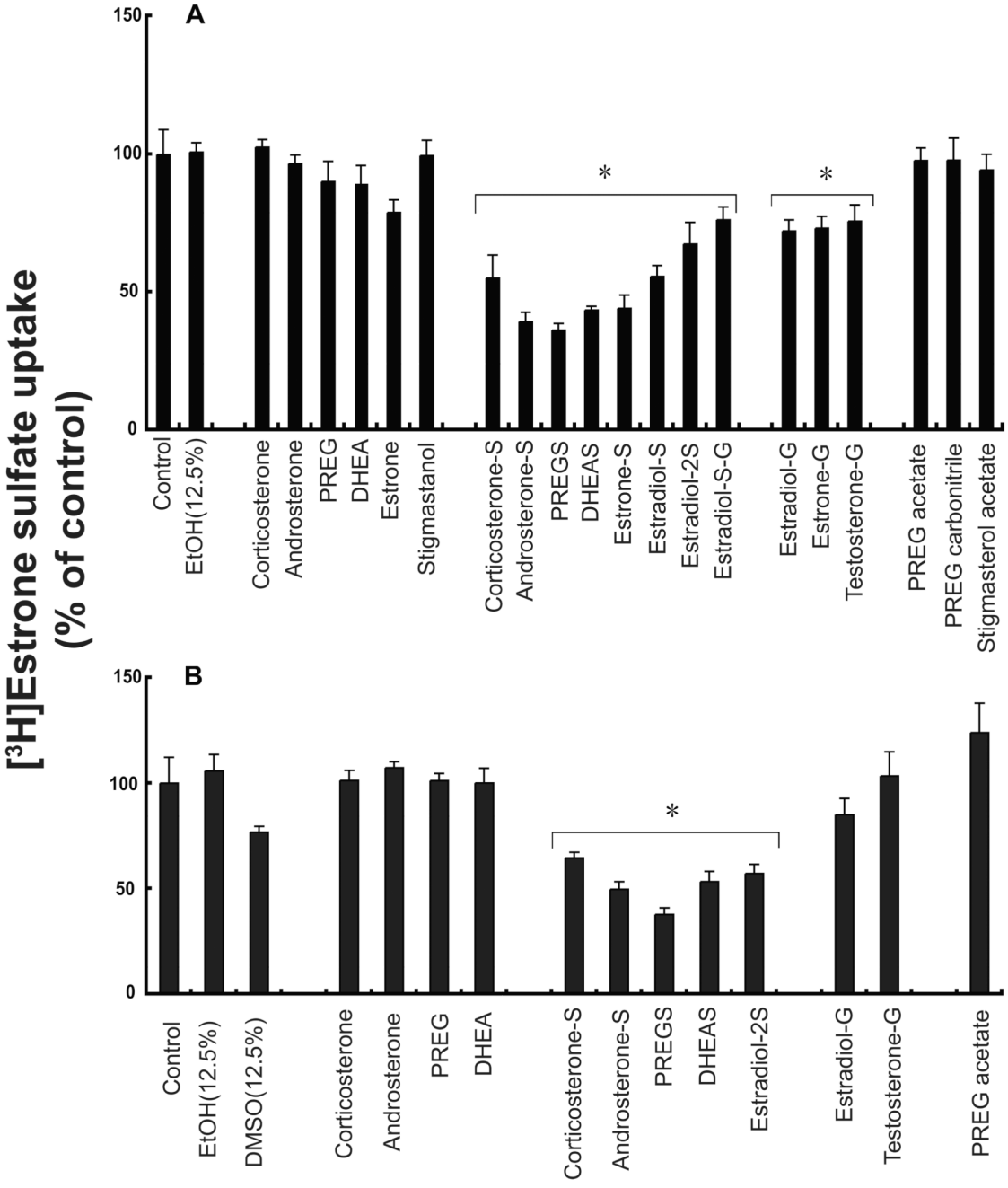

Figure 1. *Cis*-inhibition of Ostα-Ostβ- and OSTα-OSTβ-mediated [^{3}H]estrone 3-sulfate uptake by conjugated steroids

Effects of different steroids on mouse Ostα-Ostβ (A) and human OSTα-OSTβ (B) mediated transport of [^{3}H]estrone 3-sulfate. Uptake of 50 nM [^{3}H]estrone 3-sulfate was measured for 5 min in the absence (control) and presence of 12.5% ethanol and/or 500 μM of the indicated compounds. Data are expressed as a percent of the control values ± S.E. (n = 3–6 different oocyte preparations, each performed in triplicate), * $P<0.05$. (-S= sulfated; -G= glucuronidated; -2S= 2 sulfate groups; -S-G= sulfated and glucuronidated)

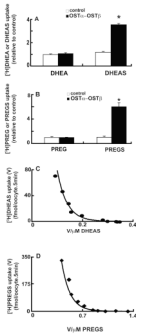

Figure 2. Human OSTα-OSTβ-mediated transport of [^{3}H]DHEAS and [^{3}H]PREGS

Uptake of 1 μM of either [^{3}H]DHEAS and [^{3}H]DHEA (A), or of [^{3}H]PREGS and [^{3}H]PREG (B) was measured for 5 min at 25°C. To define transport kinetics, oocytes were incubated with [^{3}H]PREGS (C) or [^{3}H]DHEAS (D) concentrations of 0.1, 0.33, 1, 3.3, 10, 50, 100, 200, 400, and 800 μM, and uptake was measured for 5 min at 25°C. Values are means ± S.E. of 4 experiments in distinct oocyte preparations, each performed in triplicate. For DHEAS, the Km (μM), Vmax (fmol/oocyte.5min), and Vmax/Km (nL/oocyte.5min) values of the high-affinity component were 1.5±0.4, 0.8±0.2, and 0.6±0.2, whereas for the low-affinity component they were 532±58, 101±17, and 0.19±0.03, respectively. For PREGS, the Km (μM), Vmax (fmol/oocyte.5min), and Vmax/Km (nL/oocyte.5min) values of the high-affinity component were 6.9±2.1, 9.4±1.5, and 1.5±0.2, whereas for the low-affinity component they were 909±72, 643±34, and 0.71±0.04, respectively.

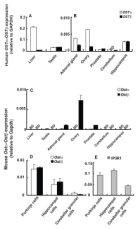

Figure 3. Human *OSTα and OSTβ* and mouse *Ostα and Ostβ* mRNA expression in brain and steroidogenic tissues

Total RNA isolated from different human (A,B) or mouse tissues (C) were subjected to quantitative real time RT-PCR analysis. *Ostα and Ost*β (C) and *IP3R1* (E) mRNA levels were also measured in specific mouse cells captured by laser capture microdissection. Data are reported relative to *GAPDH* expression for each tissue and cell. Values are means ± S.E., n=4 separate experiments.

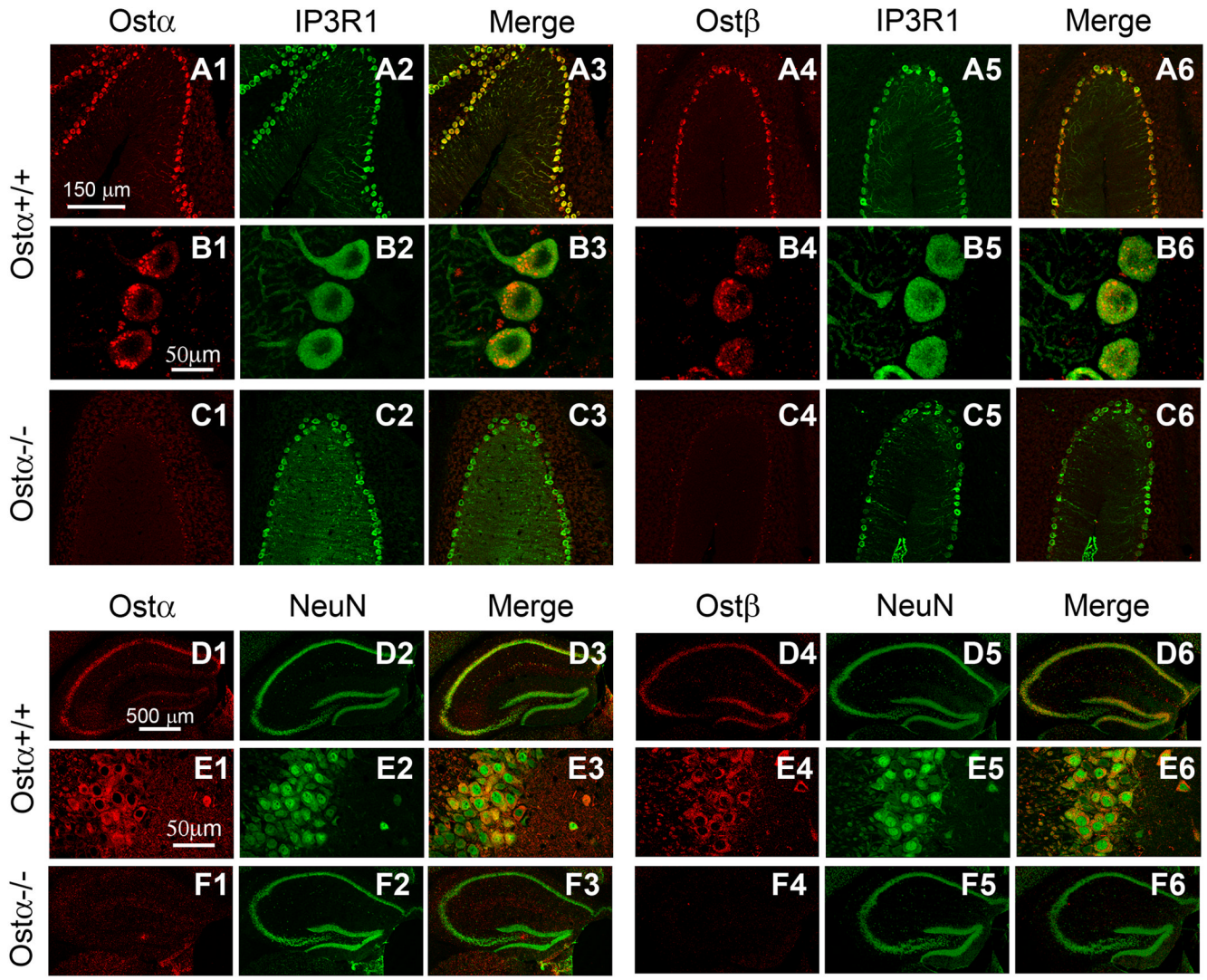

Figure 4. Immunolocalization of Ostα and Ostβ in mouse brain

Brain sections from *Ostα*$^{+/+}$ and *Ostα*$^{-/-}$ mice were labeled with anti-Ostα (panels 1–3 in rows A–F) or anti-Ostβ antibodies (panels 4–6 in rows A–F), along with antibodies to either IP3R1, a Purkinje cell marker (panels 2, 3, 5, and 6 in rows A–C), or NeuN, a neuronal marker (panels 2, 3, 5, and 6 in rows D–F).

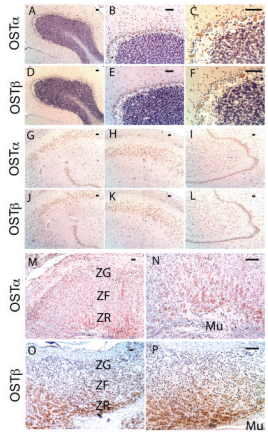

Figure 5. Immunolocalization of OSTα and OSTβ in human brain and adrenal gland

Human tissues were labeled with anti-OSTα (A–C, G–I, M, N) or anti-OSTβ (D–F, J–L, O, P) antibodies. In the adrenal gland, signals for OSTα and OSTβ were relatively strong in the *zona reticularis* (ZR) of the adrenal cortex, whereas the *zona glomerulosa* (ZG) and *zona fasciculata* (ZF) had weaker staining (M, O). Higher magnification showed that OSTα and OSTβ are expressed in cells of the *zona reticularis* (N, P). Mu = medulla; scale bar represents 100 μm.

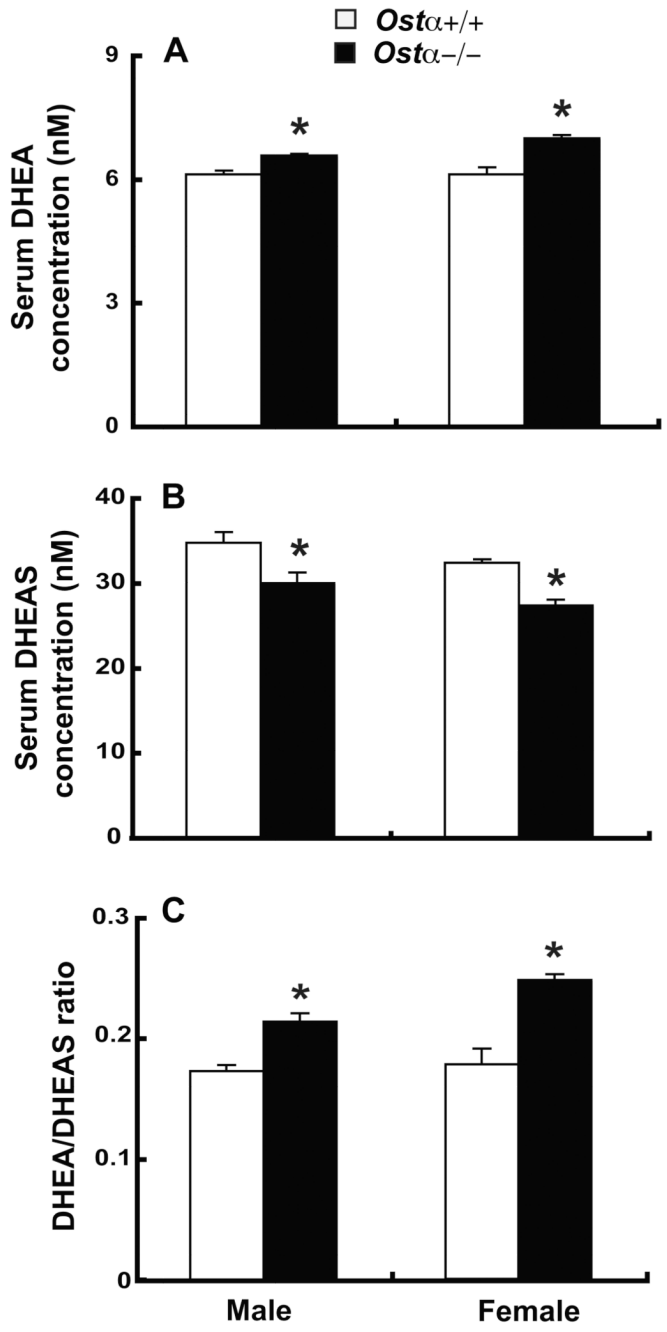

Figure 6. Serum DHEA and DHEAS levels are altered in *Ostα*-deficient mice

Serum DHEA (A) and DHEAS (B) levels were measured in male and female mice. DHEA/DHEAS ratios were also calculated (C). Values are means ± SE, n = 5–6 mice in each group; *Significantly different from $Ost\alpha^{+/+}$ animals, $P < 0.05$.

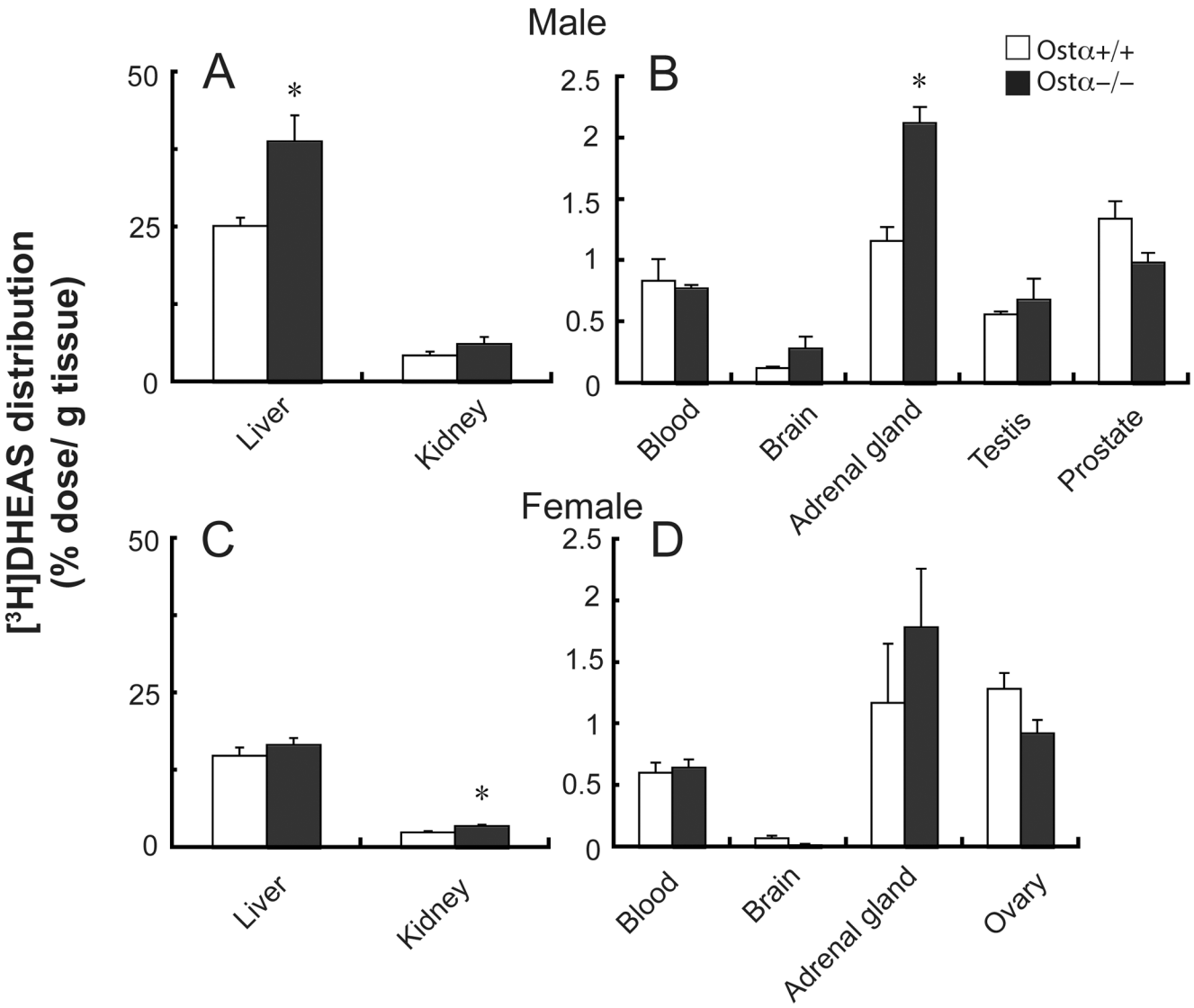

Figure 7. Altered distribution of [^{3}H]DHEAS in *Ostα*-deficient mice

Tissue distribution of radioactivity after administration of [^{3}H]DHEAS in male (A, B) and female (C, D). Mice were injected intraperitoneally with 0.4 μmol in 400 μl, and tissues collected after 2 h. Values are means ± SE, n = 3–4; *Significantly different from *Ostα*$^{+/+}$ animals, $P < 0.05$.

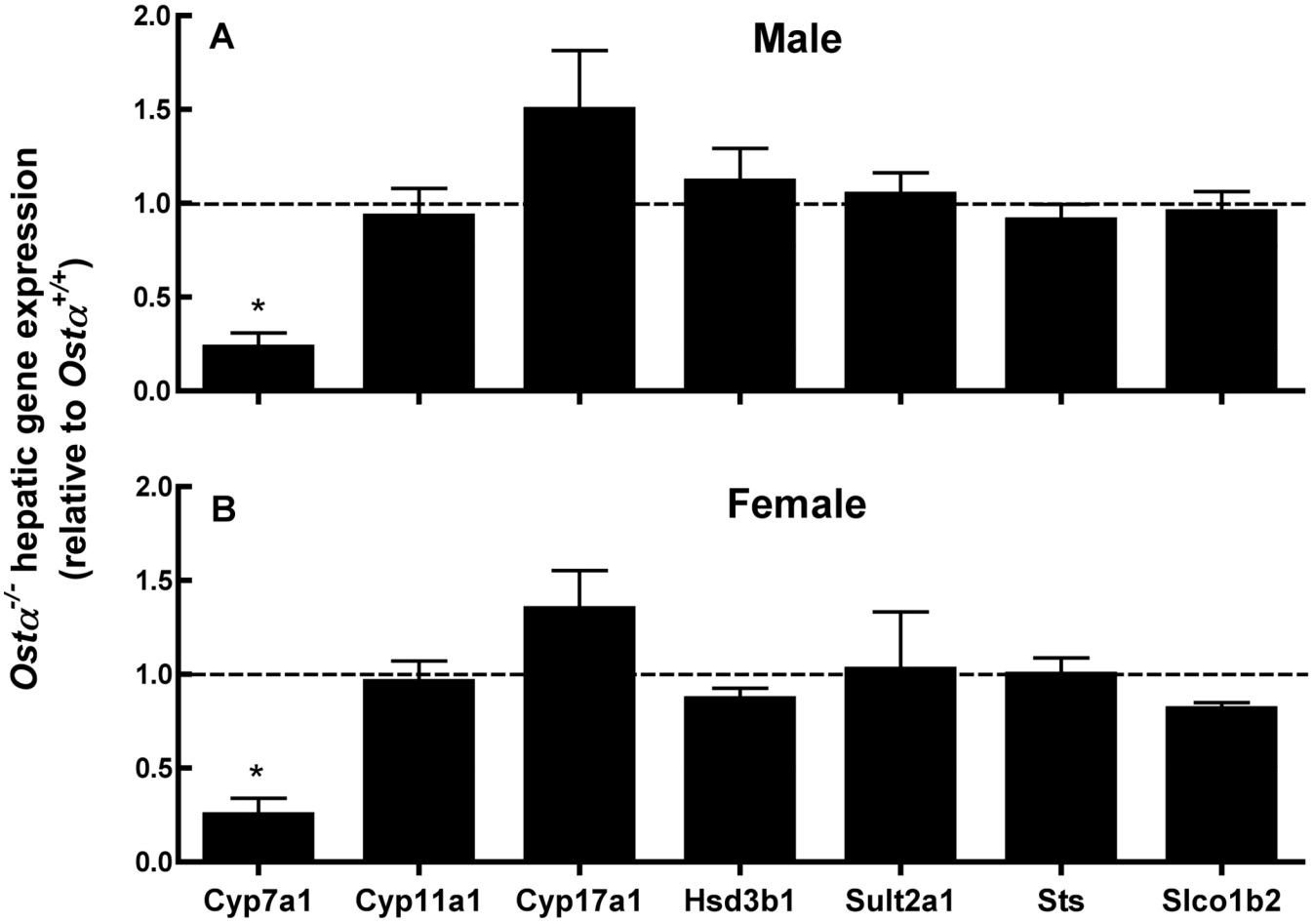

Figure 8. Hepatic expression of some of the key genes involved in cholesterol and steroid homeostasis in wild type and *Ostα*-deficient mice

Total RNA isolated from male (A) and female (B) mouse livers was subjected to quantitative real time RT-PCR analysis. Data were assessed relative to *Gapdh* expression, and are reported as a percent of the value in the $Ost\alpha^{+/+}$ mice. Values are means ± S.E., n=4–5 mice per group. *Significantly different from $Ost\alpha^{+/+}$ animals, $P < 0.05$.

Table 1

Primer sequences used for real-time RT-PCR analysis

Primer Pair	Accession Number	Temperature, C	Forward Sequence (5'-3')	Reverse Sequence (5'-3')	Amplicon Size, bp
OSTα	NM_152672	56	TGTTGGGCCCTTTCCAATAC	GGCTCCCATGTTCTGCTCAC	220
OSTβ	NM_178859	52	CAGGCAAGCAGAAAAGAAAAGATG	CCGGAAGGAAAACTGACA	187
Ostα	NM_145932	54	ATGCATCTGGGTGAACAGAA	GAGTAGGGAGGTGAGCAAGC	115
Ostβ	NM_178933	56	GACCACAGTGCAGAGAAAGC	CTTGTCATCACCACCAGGAC	125
GAPDH	NM_002046	56	AACAGCGACACCCACTCCTC	CATACCAGGAAATGAGCTTGACAA	81
Gapdh	NM_008084	57	TGTGTCCGTCGTGGATCTGA	CCTGCTTCACCACCTTCTTGAT	80
Ip3r1	NM_010585	55	GGATCTAGTTCCACAAGCAGG	TGCCTCCTTCCAGAAGTG	149
Cyp7a1	NM_007824	62	GACATGGAGAAGGCTAAGACG	CCAAGTAAATGGCATTCCCT	193
Cyp11a1	NM_019779	58	GGAGTCAGTTTACATCGTGGA	ATCACCTCTTGGTTTAGGACG	189
Cyp17a1	NM_007809	56	AGACACCTAATGCCAAGTTCC	TACCCAGGCGAAGAGAATAGA	147
Hsd3b1	NM_008293	56	AGGGCATCTCTGTTGTCATCCA	GCTGGCACACTTGCTTGAAC	136
Sult2a1	NM_001111296	56	TAGGGCCAGATGAGCTGGATCT	ACTTTATCGAAGGCTTCAGC	190
Sts	NM_009293	52	TCCTGCTCTTCCTGTCCTTCCT	TGGTCCGAGGTGAAGTAGACGA	190
Slco1b2	NM_020495	58	ACCTCACCTGAGATAATGGAG	GTTATGCGGACACTTCTCAG	287

OST/Ost, human/mouse organic solute transporter; GAPDH/Gapdh, human/mouse glyceraldehyde-3-phosphate dehydrogenase; Ip3r1, inositol 1,4,5-triphosphate receptor 1; Cyp7a1, cytochrome P450, family 7, subfamily a, polypeptide 1; Cyp11a1, cytochrome P450, family 11, subfamily a, polypeptide 1; Cyp17a1, cytochrome P450, family 17, subfamily a, polypeptide 1; Hsd3b1, hydroxy-delta-5-steroid dehydrogenase, 3 beta- and steroid delta-isomerase 1; Sult2a1, sulfotransferase family 2A, dehydroepiandrosterone (DHEA)-preferring, member 1; Sts, steroid sulfatase; Slco1b2, solute carrier organic anion transporter family, member 1b2.